ACS APPLIED NANO MATERIALS

www.acsanm.org Article

Facile Synthesis of Multicolored Stacked Quantum Dot Films for Efficient White Light Emission

Eun A Kim, Joon Yup Lee, Jisu Han, Hong Gu Kang, Minsu Kim, Jaehoon Lim, and Seong-Yong Cho*

Cite This: ACS Appl. Nano Mater. 2023, 6, 11455−11464 Read Online

ACCESS | Metrics & More | Article Recommendations | Supporting Information

ABSTRACT: Quantum dot (QD)-based white light-emitting diodes (LEDs) or white QD-LEDs were successfully fabricated by stacking QD films of primary colors (i.e., red, green, and blue). An ultrathin ZnO film was deposited between each QD layer to facilitate the formation of a tricolor-stacked QD structure. Such stacked QD films effectively suppress the Förster resonance energy transfer between QDs and enable efficient blue light emission, unlike randomly mixed QD films of different colors. The photoluminescence (PL) spectra of various QD films were obtained to study the change in the corresponding color gamut with applied voltage. In addition, QD-LEDs were fabricated based on the PL behavior and electronic band diagrams of QDs of different colors. Maximum luminance and peak EQE of white QD-LED shows 5700 cd/m^2 and 1.1% compared to 2200 cd/m^2 and 0.3% of QD-LED with mixed QD layer. Finally, a smooth color transition and white light emission were achieved using a blue/green/red stacking sequence for the QDs, which successfully suppressed the energy transfer effect. The overall performance and brightness of the white QD-LEDs synthesized in this study can be further enhanced by developing high-performance blue QDs.

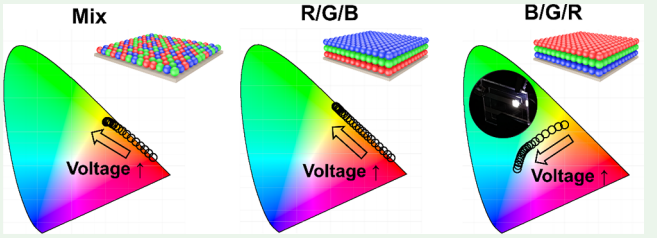

KEYWORDS: *white light emission, atomic layer deposition, ZnO, stacked QD, color gamut, diethylzinc*

INTRODUCTION

Colloidal quantum dots (QDs) are semiconductor nanocrystals that are promising materials for emissive displays owing to their excellent optoelectronic properties and ease of large-scale synthesis.[1−5] QDs can emit a wide range of wavelengths in the visible spectrum depending on their size and composition. The photoluminescence (PL) quantum yield of QDs has been optimized to reach unity for the primary colors (i.e., red (R), green (G), and blue (B)) owing to the advancement in synthetic parameter control and the optimization of device architecture.[6−10] QDs are typically incorporated into multilayer thin films for optoelectronic applications, such as light-emitting diodes (LEDs),[9,11,12] photodetectors,[13,14] and light-emitting transistors.[15,16] Unicolor QD-LEDs have been fabricated for self-emissive display applications; in addition, QDs have been used to generate white light.[17−23] In particular, high-brightness white QD-LEDs can be used as backlight units, as well as for outdoor lighting applications.[24−26]

White light emission has been achieved by mixing QD solutions of different colors and spin-coating them in a single step.[19,27] However, the light emitted in this case is significantly red-shifted owing to the Förster resonance energy transfer (FRET) that occurs between QDs of different colors. In general, QDs of two or three different colors are randomly mixed to generate condensed films; however, red QDs (or R-QDs) typically absorb light of shorter wavelengths. Additionally, when QDs with different energy band gaps are mixed in a single film, the QD with the smaller band gap exhibits a lower turn-on voltage than those of green and blue under electrical excitation. This difference can be alternatively understood as the different exciton generation rate at a bias. Thus, exciton generation is mainly focused on the red QDs, not the green or blue QDs. In addition to this intrinsic problem, the bias-dependent exciton generation rate for each QD leads to complicated device characteristics for white QD-LEDs.

This issue can be resolved by sequentially depositing QD layers of different colors and separating them from each other. However, QDs are easily dissolved by organic solvents owing to their lack of solvent resistance.[22,28−30] Although a tandem structure formed by inserting a charge generation layer can be used to fabricate high-efficiency single-color or white QD-LEDs, this significantly increases the driving voltage and complicates the device structure.[17,23,31,32] The FRET effect can be suppressed by sequentially depositing layers of R-QDs, green QDs (or G-QDs), and blue QDs (or B-QDs) to obtain white QD-LEDs. Direct spin-casting of the QD solution onto a precoated QD film is not preferred because of the interfacial

Received: April 4, 2023
Accepted: June 2, 2023
Published: June 15, 2023

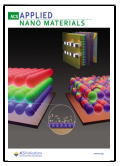

https://doi.org/10.1021/acsanm.3c01485
ACS Appl. Nano Mater. 2023, 6, 11455−11464

mixing between the different types of QDs. To ensure solvent resistance during the spin-casting of one QD layer onto a preexisting QD layer, ultrathin films composed of ZnO nanoparticles (NPs) can be deposited.[21,29] Atomic layer deposition (ALD) can be used to form an extremely thin passivation layer of ZnO on top of the QD film, such that even a single pulse of diethylzinc (DEZ) precursor can effectively cross-link the QDs on the film surface, as demonstrated in our previous studies.[33,34]

In this study, a ZnO layer was inserted between two or more QD films via ALD to suppress the FRET effect and achieve white light emission for a wide range of operating voltages without significantly affecting the charge transport. In addition to this, stacking QDs with different emission colors by ALD ZnO efficiently controls the exciton recombination zone by changing the stacking sequence of R-, G-, and B-QD films. In a randomly mixed QD film, the B-QD film rarely emits due to the higher turn-on voltage and lower exciton generation rate with accelerated FRET via a small distance with R- and G-QDs. The color balance and efficiency for different device architectures were compared, including randomly mixed and sequentially stacked QD films. A B/G/R stacking sequence for the QDs was chosen for efficient white light emission. This device structure suppressed the FRET effect more effectively than the randomly mixed film structure; moreover, the exciton recombination zone for the sequentially stacked structure spanned the entire emission layer.

EXPERIMENTAL SECTION

Synthesis of QDs. Red light-emitting CdSe/CdS/CdZnS core/shell (C/S) QDs were synthesized using the one-pot procedure described by Borg et al.[35] Green light-emitting CdZnSeS/ZnS C/S QDs were synthesized using the one-pot procedure described in our previous studies,[33,36] and blue light-emitting CdZnS/ZnS C/S QDs were prepared using the procedure described by Bae et al.[7] Transmission electron microscopy (TEM) images of each C/S QDs in this work are given in Figure S1.

Stacking of QD Films via ALD of ZnO. First, a QD film of a particular color was deposited onto a glass substrate. Next, the substrate was placed in an ALD chamber at 130 °C, where DEZ and water were used as the precursor and reactant, respectively. The pulsing and purging times used for DEZ were 0.1 and 15 s, respectively. For water, the pulsing time was kept the same, but the purging time was 50 s due to its high boiling point. To stack the different QD films, first, 10 cycles of ALD of ZnO were performed; subsequently, the QD films of the remaining colors were stacked onto the predeposited QD film. Cross-sectional TEM image of white QD-LED that includes a stacked B/G/R QD is shown in Figure S2.

Device Fabrication. To fabricate stacked QD-LEDs, first, the prepatterned indium tin oxide (ITO) substrate was sequentially cleaned with acetone, ethanol, and isopropyl alcohol. Next, the substrate was treated with UV ozone for 15 min to create a hydrophilic surface and modify the work function of ITO. Poly(3,4-ethylenedioxythiophene):poly(styrenesulfonate) (PEDOT:PSS) was used as the hole injection layer (HIL) and spin-coated onto the substrate at 4000 rpm for 30 s. Subsequently, the substrate was baked at 120 °C for 5 min in the air to evaporate water and then again at 210 °C for 10 min in a N_2-filled glovebox. The hole transport layer (HTL) was composed of Poly[(9,9-dioctylfluorenyl-2,7-diyl)-co-(4,4′-(N-(4-*sec*-butylphenyl)diphenylamine)] (TFB) (5 mg) and 2,3,5,6-Tetrafluoro-7,7,8,8-tetracyanoquinodimethane (F_4TCNQ) (1 mg) was used as a dopant in xylene and spin-coated onto the HIL at 3000 rpm for 30 s, followed by annealing at 180 °C for 30 min. A multicolored emissive layer (EML) was formed by depositing B/G/R QDs sequentially at the optimized concentrations of 16.5, 7, and 10 mg/mL, respectively. (Detailed concentrations of QDs are given in Table 1). First, the B-QDs were deposited onto the HTL, following which ALD of ZnO was performed. Next, the G-QDs were deposited onto the ZnO-coated layer of B-QDs, and finally, the R-QDs were deposited onto the layer of G-QDs after the ALD ZnO process. Spin-coating was performed at 2000 rpm for 30 s, and annealing was performed at 180 °C for 30 min, for all three QD layers. The electron transport layer (ETL) was composed of a ZnO NP solution with a concentration of 30 mg/mL, which was spin-coated onto the substrate at 2000 rpm for 30 s and baked at 110 °C for 30 min. An Al cathode of thickness 100 nm was deposited onto the substrate using a thermal evaporator. Finally, to enhance the lifetime of the QD-LED and measure its performance, the substrate was encapsulated with epoxy (NOA 8610 B) and a glass coverslip.

Table 1. QD Concentration in the Bicolor and Tricolor QD Films

		concentration of QDs (mg/mL)		
final color		red	green	blue
bicolor	yellow	20	14	
	magenta	10		30
	cyan		10	25
tricolor	white	10	7	20

Characterizations. The PL spectra of the QDs were obtained using FC2-LED (Prizmatix). The UV−visible absorbance of the QDs was measured using a DH-2000-BAL light source. The energy levels of the films were analyzed using ultraviolet photoelectron spectroscopy (UPS), which was performed using the Thermo Fisher Scientific Nexsa for a sample bias of −10 V. The time-resolved PL was measured using the Horiba FluoroMAX Plus-C spectrofluorometer. Various device characteristics, such as current density, luminance, EQE, electroluminescence (EL) intensity, and CIE coordinates were recorded using the CS-2000 spectroradiometer (Konica Minolta) and Keithley 2400B.

RESULTS AND DISCUSSION

Figure 1a illustrates the method used to stack the QDs of different colors using ALD. The QD layers of different colors were deposited sequentially via spin-casting. ALD of ZnO facilitated the surface cross-linking of the QDs, which occurred within 10 cycles of ALD (i.e., < 2 nm thick ZnO layer) when the QD surface was treated with a DEZ precursor. This process yielded stacked QD layers of different colors. Unlike the QD films synthesized from a solution of QDs of different colors, the ZnO-coated preexisting QD layer was not damaged during the spin-casting of an additional QD layer. Yang and co-workers reported that spin-casting of an ultrathin film of ZnO NPs can provide solvent resistance to QD films and enable the stacking of multiple QD layers.[21] However, we believe that ALD can be used to deposit an even thinner layer (i.e., submonolayer) of ZnO. Moreover, ALD enhances the performance of QD-LEDs, as shown in our previous studies.[33,34,36] In contrast to ZnO NPs that have surface defects and can cause PL quenching of QDs,[12] ALD of ZnO enhances the PL intensity of QDs. Figure S3 illustrates the PL spectra improvement of QD films for each primary color following the application of ultrathin ALD ZnO. When ALD of ZnO was not performed, the precoated G-QD film was easily damaged during spin-casting of the R-QDs, as shown in Figure 1a. However, when a ZnO layer was coated onto the G-QD film via ALD, a uniform bilayer of R- and G-QDs was obtained. Figure 1b illustrates a stacked multicolored QD device fabricated using ALD, which functions as a white QD-LED. The magnified image shows the detailed structure of the

https://doi.org/10.1021/acsanm.3c01485
ACS Appl. Nano Mater. 2023, 6, 11455−11464

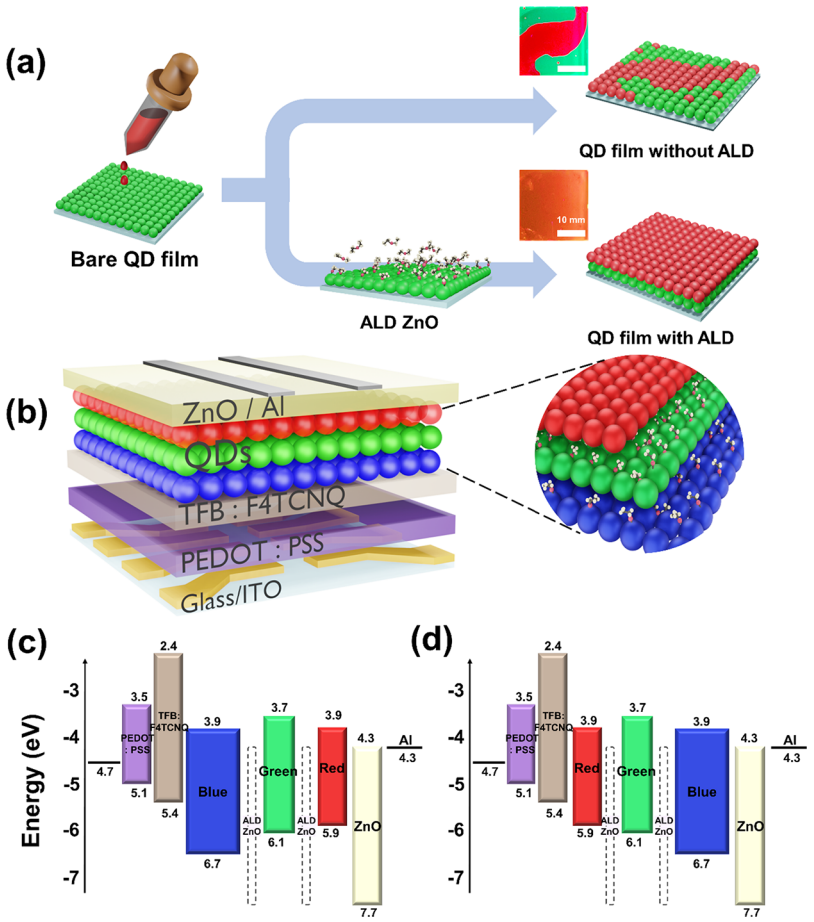

Figure 1. (a) Schematic illustration of the stacking of QD films of different colors with (lower) and without (upper) ALD of ZnO. The insets show the photographs of the stacked QD films. (b) Structure of the QD-LED with stacked QD layers, and the magnified image demonstrates the cross-linking of the QDs in the precoated QD layers. (c) Energy band diagrams of (c) B/G/R stacked QD-LED and (d) R/G/B stacked QD-LED.

multicolored QD layers with a B/G/R stacking sequence from bottom to top, as well as the DEZ molecules that cross-link the QDs. Thus, QD layers of different colors can be sequentially deposited using a ZnO interlayer to achieve white light emission. Figure S2 shows a TEM image of white QD-LED in this work and the stacked QD film shows no detectable formation of ZnO between QDs with different emission colors. The thickness of each QD layer was modified systematically to achieve color balance and white light emission for a wide range of applied voltages. Figure 1c,d shows the electronic band diagrams of the white QD-LEDs developed in this work. Stacked multilayers of R/G/B (or B/G/R) QD films were inserted between the PEDOT:PSS/TFB:F_4TCNQ HIL/HTL and ZnO ETL. The valence and conduction bands of the charge transport layers and QDs were determined using UPS data, as shown in Supporting Information Figure S4 and the literature.[11,37,38]

Before stacking the R/G/B QD films to fabricate white QD-LEDs, it is necessary to optimize the ratio of the different colors of QDs. To understand the effect of combining QDs of two or more colors, the PL spectra of the mixed and stacked QD films were compared, as shown in Figure 2. The absorbance and PL spectra of the unicolor R-, G-, and B-QD films are shown in Figure 2a, which shows that the emission of the B-QDs would be absorbed by the G- and R-QDs. Note that the R-QDs would absorb the emission by both the B- and G-QDs owing to their spectral overlap. The PL spectra of the bicolor and unicolor QD films are compared in Supporting Information Figure S5. The exact concentrations of the QDs in the bicolor and tricolor QD films are listed in Table 1. Figure 2b shows the PL spectra of the stacked and mixed R/G/B QD films, and the insets show the corresponding photographs. The mixed tricolor QD film exhibited significantly stronger red and green light emissions than the stacked tricolor QD film owing to the FRET effect. This can be further confirmed using the time-resolved PL lifetime data presented in Supporting Information Figure S6 and Table 2. The PL lifetime of the randomly mixed R-QDs in the condensed film state is much longer than that of the R-QDs in the stacked QD film. Conversely, the PL lifetime of the B-QDs in the mixed QD film is much shorter than that of the B-QDs in the stacked QD film. These results clearly indicate that a significant amount of energy transfer occurs in the randomly mixed R/G/B QD film compared to that in the sequentially stacked R/G/B QD film. A mixed R/G QD film was prepared by randomly mixing R-QDs (20 mg/mL) and G-QDs (14 mg/mL) and spin-casting the solution in a single step. Additionally, stacked R/G and G/R QD films were prepared by first spin-casting a QD layer of a particular color, followed by ALD of ZnO, and finally spin-coating the second QD layer of a different color. The PL spectra and photographs of the mixed and stacked R/G QD films are presented in Figure 2c. The mixed R/G QD film exhibited the weakest green light emission and an overall orangish color, owing to the enhanced FRET effect. By

https://doi.org/10.1021/acsanm.3c01485
ACS Appl. Nano Mater. 2023, 6, 11455−11464

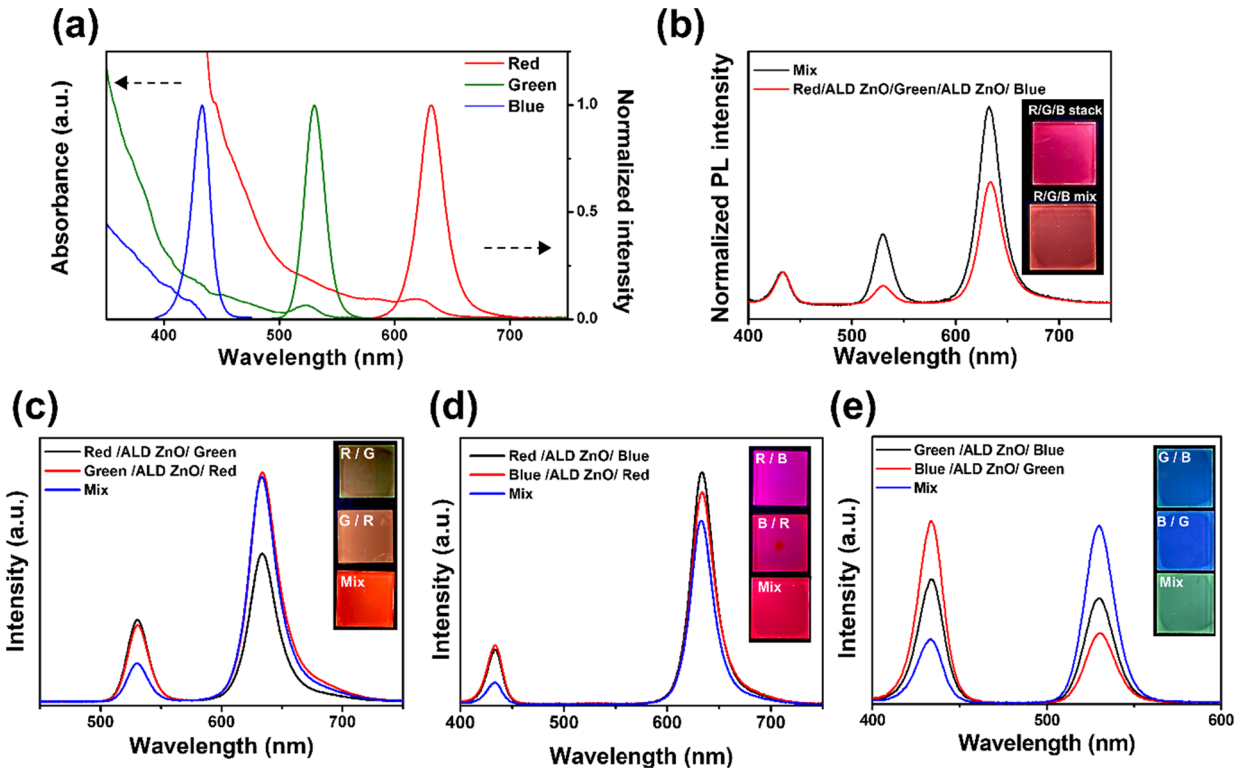

Figure 2. (a) Absorbance and normalized PL spectra of R, G, and B QD solutions. (b) PL spectra of tricolor stacked and mixed QD films. The insets show the photographs of the tricolor QD films. PL spectra of bicolor stacked and mixed QD films: (c) R/G, (d) R/B, and (e) G/B.

Table 2. Average PL Lifetime Constant (ns) of R-, G-, and B-QDs in the Mixed and Stacked Bicolor and Tricolor Films

			bicolor		tricolor
		yellow	magenta	cyan	white
red	stacked	11.51	9.75		8.11
	mixed	11.76	12.4		10.6
green	stacked	4.35		9.41	4.31
	mixed	3.03		11.3	3.64
blue	stacked		4.85	5.66	2.71
	mixed		1.3	4.35	1.73

contrast, the stacked R/G QD film exhibited a strong green light emission and hence a comparatively greener color. The mixed and stacked R/B and G/B QD films exhibited a similar behavior, as shown in Figure 2d,e, respectively. Despite a relatively higher concentration of B-QDs (30 mg/mL) than R-QDs (10 mg/mL), the mixed B/R QD film appeared almost red in color due to a significant amount of energy transfer, as shown in Figure 2d. By contrast, both the stacked R/B and B/R QD films exhibited a strong blue light emission, as shown by the corresponding spectra and photographs (inset) in Figure 2d. The stacked G/B QD film exhibited a stronger blue light emission than the mixed G (10 mg/mL)/B (25 mg/mL) QD film.

Unlike the PL spectra of the stacked QD films (which exhibit a strong FRET effect), the relative and normalized EL spectra of the mixed and stacked QD films are notably different, as shown in Figure 3a–f for mixed and stacked R/G QD films (for the results corresponding to R/B and B/G QD films, see Supporting Information Figures S7 and S8). Figure 3g–i shows the CIE color indices of the mixed and stacked R/G QD films, which demonstrate the variation of color with operating voltage. For an operating voltage of 3.8 V, the mixed R/G QD film exhibited predominantly red light emission, as shown in Figure 3a. This is consistent with the corresponding PL spectrum of the mixed R/G QD film, as shown in Figure 2c. When the applied bias was increased to 7.4 V, the emission from the G-QDs enhanced significantly. However, the overall emission color remained in the red region of the CIE diagram, as shown in Figure 3g. It is important to consider the stacking sequence of the QD films when fabricating stacked QD-LEDs. For instance, for the R/G stacked QD-LED, as shown in Figure 3b, the emission color was predominantly red at all operating voltages. The intensity of green light emission was extremely low, and the overall emission color was located in the red region of the CIE diagram, as shown in Figure 3h. Yang and co-workers investigated the effect of different stacking sequences on multilayer QD films with a ZnO NP interlayer.[20] In a typical QD-LED, charge transport is often unbalanced owing to faster electron transport and higher hole injection barriers.[39,40] Therefore, the exciton recombination zone is more likely to be located near the interface between the HTL and QD film rather than at the exact center of the EML.[37,41] Consequently, a G/R stacking sequence (i.e., R-QDs deposited on top of G-QDs) is preferred because it facilitates light emission from the QDs with a larger bandgap. Once the holes are injected from the HIL/HTL into the EML of the QDs with the larger bandgap, the exciton recombination zone can extend across both the R- and G-QD layers owing to the absence of additional charge injection barriers.[42] A more balanced color emission between red and green can be achieved by applying a higher voltage to facilitate more charge injection into the G-QD layer. Thus, a gradual transition from red to green emission color was successfully achieved by adopting a G/R stacking sequence for the QD films, as demonstrated by the

https://doi.org/10.1021/acsanm.3c01485
ACS Appl. Nano Mater. 2023, 6, 11455−11464

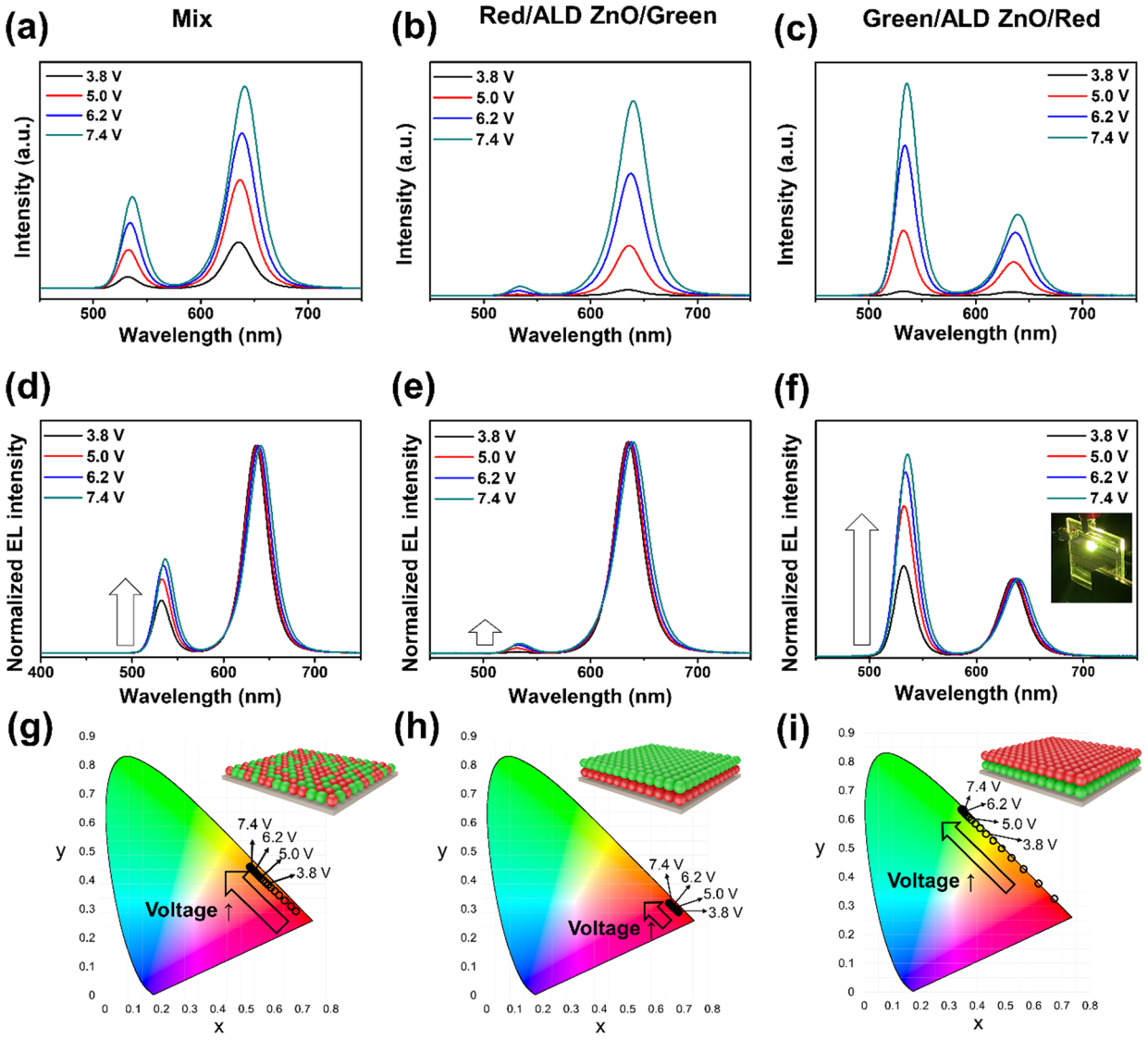

Figure 3. Color characteristics of mixed and stacked R/G QD-LEDs for different applied voltages. Relative EL spectra of: (a) mixed, (b) R/G stacked, and (c) G/R stacked QD films. (d–f) Normalized EL spectra with respect to red light emission corresponding to (a)–(c), respectively. CIE color gamut of (g) mixed, (h) R/G stacked, and (i) G/R stacked QD films. The insets show the schematic structures of the bicolor QD films.

inset in Figure 3f and CIE diagram in Figure 3i. EL spectra of QD-LEDs at each applied bias and PL spectra of mixed and stacked G/R QD films are shown in Figure S9. A similar color variation with operating voltage was observed for the R/B and G/B QD-LEDs, as shown in Supporting Information Figures S7 and S8.

Figure 4 presents the current density, luminance, and EQE values of different mixed and stacked bicolor QD-LEDs. Figure 4a shows the current density and luminance as functions of applied voltage and Figure 4b shows the EQE as a function of current density for the mixed and stacked R/G QD-LEDs. The stacked G/R QD-LED demonstrated the highest luminance (65,000 cd/m^2) and EQE across the entire range of applied voltage and current density, respectively. Hole injection into the G-QD layer resulted in a high-brightness G/R QD-LED, as also demonstrated by the energy band diagrams in Figure 1c,d. Although the mixed R/G QD film exhibited the highest current density because of its smaller thickness compared to that of the stacked bilayer films, it exhibited the lowest EQE. Figure 4c shows the current density and luminance and Figure 4d shows the EQE of the mixed and stacked R/B QD-LEDs. The stacked R/B QD-LED demonstrated the highest luminance, which can be attributed to the higher sensitivity of the photopic function to red light, as well as the fact that the R-QD film was located closer to the HTL and exciton recombination zone in this case. The stacked B/R QD-LED exhibited the lowest brightness across the entire voltage range owing to the relatively low performance of the B-QDs. However, this QD-LED exhibited the highest EQE and lowest current density owing to the significantly large energy bandgap of the B-QDs. The G/R QD-LEDs shown in Figure 4e,f exhibited a slightly different behavior owing to the significant difference between the performance of the B- and G-QDs. Specifically, the G-QDs have a higher brightness and smaller electronic bandgap than the B-QDs. Consequently, the stacked G/B QD-LED exhibited the highest current density owing to the smaller bandgap of the G-QDs and the highest luminance because of the higher brightness of the G-QDs (owing to their proximity to the exciton recombination zone). When the B-QDs were located near the exciton recombination zone, the

https://doi.org/10.1021/acsanm.3c01485
ACS Appl. Nano Mater. 2023, 6, 11455–11464

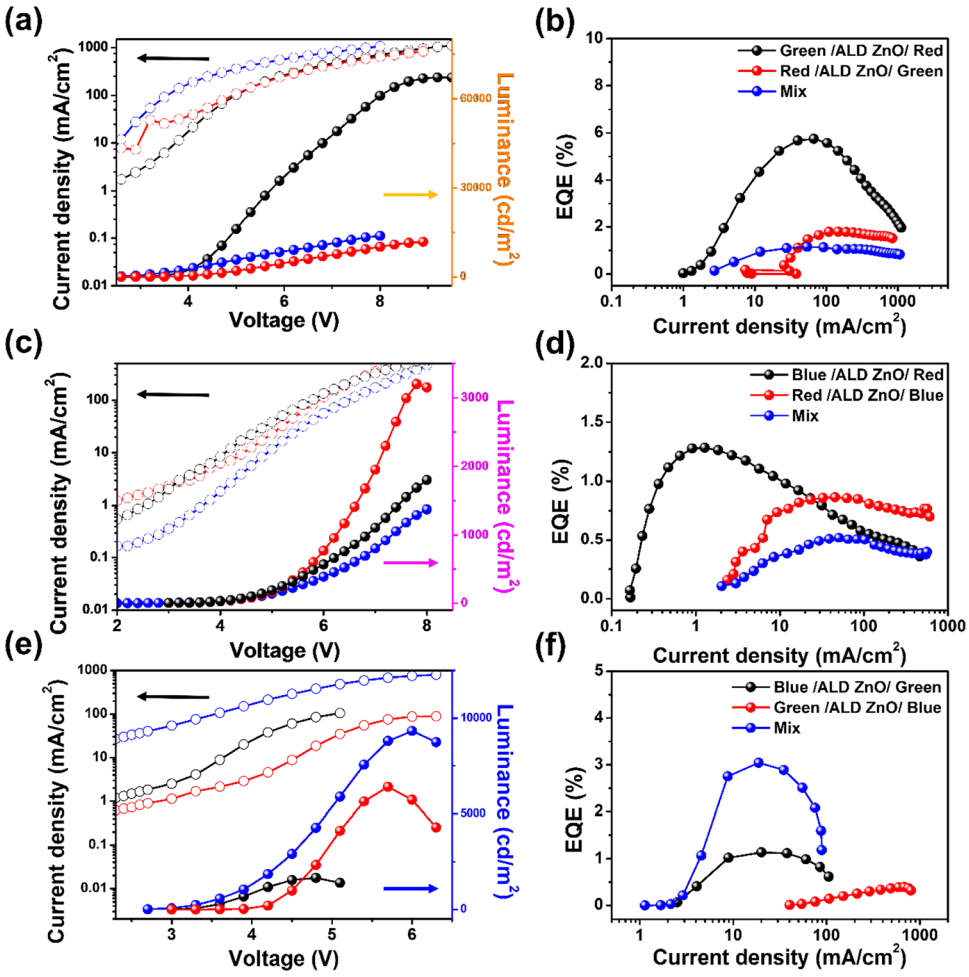

Figure 4. Current density (open circles) and luminance (closed circles) as functions of applied voltage: (a) R/G QD films, (c) B/R QD films, and (e) B/G QD films. EQE as a function of current density: (b) R/G QD films, (d) B/R QD films, and (f) B/G QD films.

brightness of the stacked B/G QD-LEDs reduced significantly owing to the relatively lower performance of the currently developed B-QDs compared to that of the R- and G-QDs. The performance of LEDs based on unicolor R-, G, and B-QDs is shown in Supporting Information Figure S10. Note that the stacked B/G QD-LED exhibited a significantly lower EQE than the mixed B/G QD LED. This is because in the mixed QD-LED, both the G- and B-QDs were located near the exciton recombination zone. The color characteristics of the bilayer QD films are summarized in Supporting Information Figure S11.

To fabricate a white QD-LED, the R-, G-, and B-QD layers were sequentially deposited after the QDs were cross-linked via ALD of ZnO. Figure 5a–f shows the relative and normalized EL spectra of the mixed, R/G/B stacked, and B/G/R stacked QD-LEDs. Figure 5g–i presents the CIE diagrams of the mixed, R/G/B stacked, and B/G/R stacked QD-LEDs, respectively, for different applied voltages. For the mixed tricolor QD-LED, the emission color was predominantly red at lower operating voltages and yellow at higher voltages, as shown in the corresponding CIE diagram. Interestingly, blue light emission was significantly low even at 7.5 V. This indicates that either electrical excitation occurred mostly in the low-bandgap QDs, or significant energy transfer occurred between the blue and other QDs. A higher operating voltage shifted the emission color in the CIE diagram to the yellow regime. In addition, the normalized EL spectra of the mixed tricolor QD-LED exhibited significant green light emission, but white light emission was not achieved. The R/G/B stacked QD-LED shown in Figure 5b,e,h, exhibited a similar color variation with voltage as that of the mixed tricolor QD-LED, except that no blue light emission was observed. This is because the large-bandgap B-QD layer is too far from the exciton recombination zone, and hence, even a high operating voltage is not sufficient to induce charge injection into this layer. Thus, the overall color behavior of the R/G/B stacked QD-LED resembled that of the R/G stacked QD-LED (i.e., without the B-QDs), as shown in Figure 3. However, the color transition from red to green in the R/G/B stacked QD-LED was smoother than that in the mixed tricolor QD-LED. The B/G/R stacked QD-LEDs shown in Figure 5c,f,i successfully emitted white light. A dynamic color change was observed across the entire CIE diagram due to the optimized energy bands of the stacked QD structure and suppressed FRET effect. Thus, white light emission could be achieved by suppressing the FRET effect and placing the larger-bandgap B-QDs close to the exciton recombination zone. The inset in Figure 5f shows a photograph of the white QD-LED composed of stacked B/G/R QD layers.

Figure 6 presents the current density, luminance, and EQE data of the mixed and stacked tricolor QD-LEDs. Although white light emission was achieved by the B/G/R stacked QD-

https://doi.org/10.1021/acsanm.3c01485
ACS Appl. Nano Mater. 2023, 6, 11455−11464

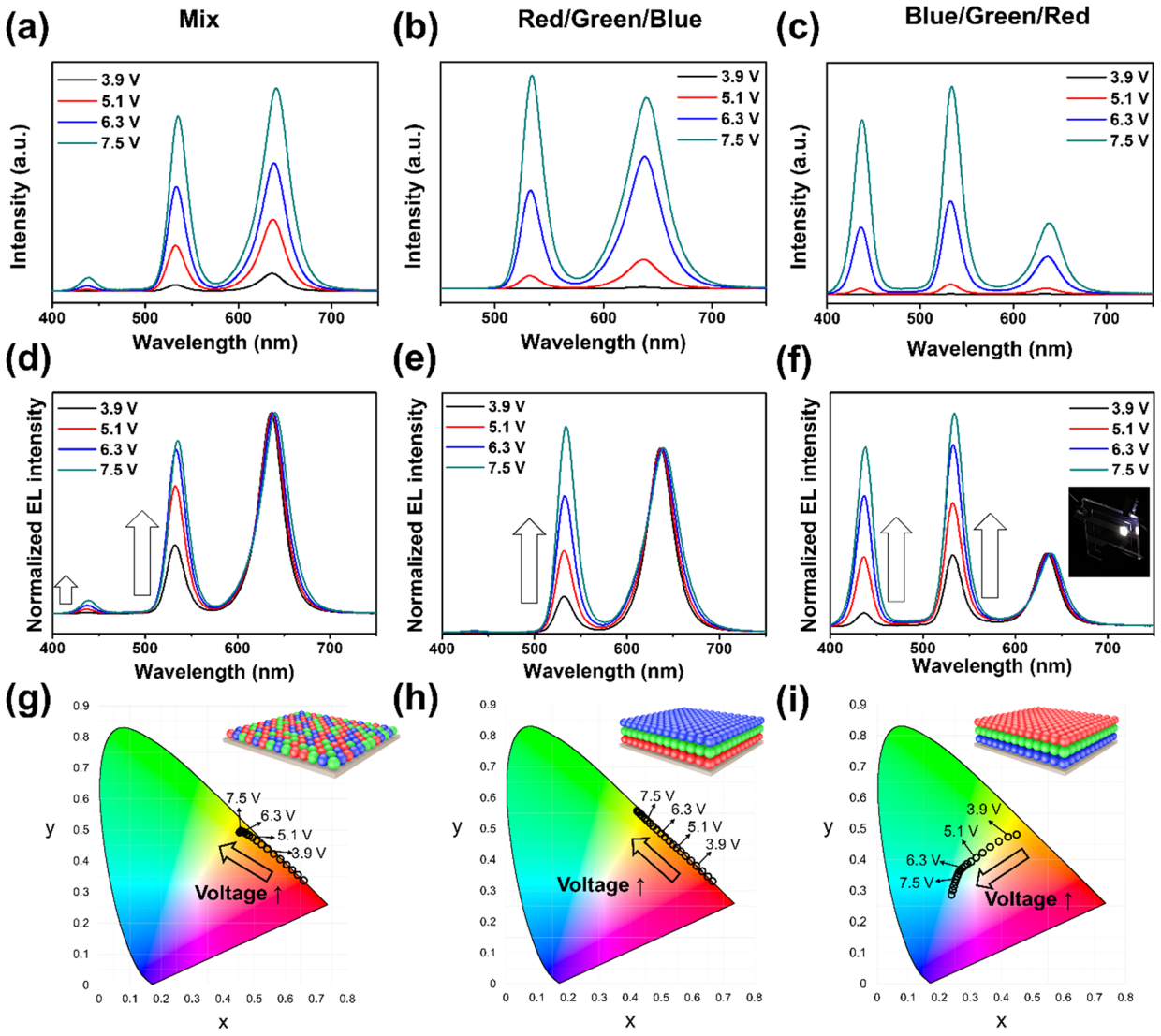

Figure 5. Color characteristics of mixed and stacked tricolor QD-LEDs for different applied voltages. EL spectra of (a) mixed, (b) R/G/B stacked, and (c) B/G/R stacked QD films. (d–f) Normalized EL spectra corresponding to (a–c), respectively. CIE color gamut of (g) mixed, (h) R/G/B stacked, and (i) B/G/R stacked QD films. The insets show the schematic structures of the tricolor QD films.

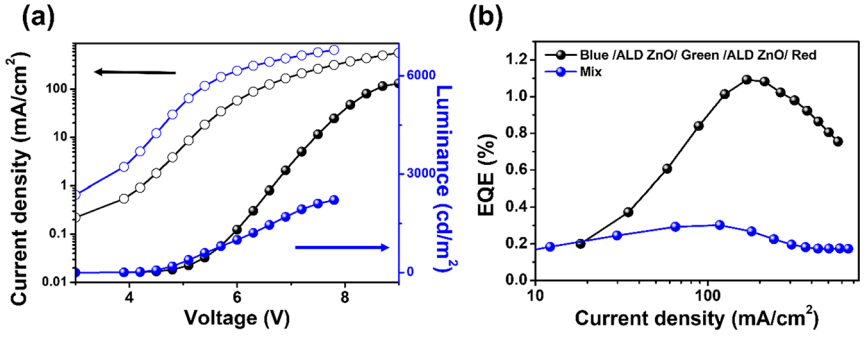

Figure 6. (a) Current density (open circles) and luminance (closed circles) as functions of operating voltage and (b) EQE as a function of current density, for the mixed and stacked tricolor QD-LEDs.

LED, the highest brightness was exhibited by the R/G/B stacked QD-LED, as shown in Figure S12. Unlike the successful color change and white emission of the B/G/R QD-LED, the highest brightness of tricolor QD-LED is achieved by R/G/B stacked QD films. This can be attributed to the relatively poor performance of the B-QDs. The high EQE of the R/G/B stacked QD-LED is because of the contribution of the green light emission to the luminance for a high applied bias, as shown in Figure 5e. However, no blue light emission was observed at high voltages. In case of the B/G/R stacked QD-LED, although a gradual change in emission color with applied bias was observed (see Figure 5f,i), an

https://doi.org/10.1021/acsanm.3c01485
ACS Appl. Nano Mater. 2023, 6, 11455–11464

increase in the blue light emission suppressed the overall luminance due to the low brightness of the B-QDs. The CIE indices of 10 white QD-LEDs at 3, 4, and 5 V are presented in Figures S13 and S14 to understand the statistical analysis on white QD-LED formation. It is evident that all the white QD-LEDs exhibit similar trends as the applied voltage increases. The ranges of x and y indices for each bias are depicted in Figure S14c−e. Finally, the device lifetime of white QD-LEDs was measured, as shown in Figure S15. A white QD-LED with a mixed QD layer exhibits a gradual decrease in luminance and a continuous shift toward red in terms of color index. In contrast, a white QD-LED with a stacked B/G/R QD layer experiences sudden failure and an initial color index change toward the green regime. This suggests that the green QD is effectively positioned in the exciton recombination zone. As the green QD is consumed, the color index shifts toward blue and then continues to shift toward red. The long-term stability of white QD-LEDs can be enhanced by optimizing the green and blue QDs in comparison to red QDs, which have a longer lifetime and can help slow down the degradation of QDs near the recombination zone.

CONCLUSIONS

In this study, ALD of ZnO was performed to cross-link the QDs so that QD layers of different colors could be stacked without mixing QDs. The effect of different QD stacking sequences on the exciton recombination zone and FRET between QDs of different colors was studied. In addition, the PL and EL spectra of bilayer R/G, G/B, and B/R QD films were obtained. Finally, an efficient tricolor QD-LED was developed, which exhibited a continuous color transition from red to blue and successfully emitted white light for a suitable range of applied voltage. However, the overall performance and brightness of the white QD-LED fabricated in this work can be enhanced by developing high-performance B-QDs in the near future.

ASSOCIATED CONTENT

Supporting Information

The Supporting Information is available free of charge at https://pubs.acs.org/doi/10.1021/acsanm.3c01485.

UPS spectra of R-, G-, and B-QD film; PL intensities of single color, bicolor QD films; time-resolved PL data of single color, bicolor, and tricolor QD films; QD-LED device characteristics of bicolor (R/B, B/G) QD film; QD-LED device characteristics of single color QD film; EL spectra of mixed and stacked G/R QD-LED; current density (line) and luminance (dash); normalized EL intensities of bicolor QD stacked devices; current density (black line) and luminance (blue line); color coordinate variations on the CIE graph; X-index and Y-index on the CIE color diagram; device lifetime curve of QD-LED with mixed and stacked QD layer; comparison of bicolor stack and mixed QD and tricolor stack; mixed QD-LED devices; CIE coordinates of bicolor stack and mixed QD and tricolor stack and mixed QD at different voltages; summary of the performance of white-QD-LEDs are given in the Supporting Information (PDF)

AUTHOR INFORMATION

Corresponding Author

Seong-Yong Cho − *Department of Photonics and Nanoelectronics, Hanyang University ERICA, Ansan 15588, Republic of Korea;* orcid.org/0000-0001-6948-171X; Email: seongyongcho@hanyang.ac.kr

Authors

Eun A Kim − *Department of Materials Science and Engineering, Myongji University, Yongin 17058, Republic of Korea*

Joon Yup Lee − *Department of Materials Science and Engineering and Department of Semiconductor Engineering, Myongji University, Yongin 17058, Republic of Korea*

Jisu Han − *Department of Energy Science and Center for Artificial Atoms, Sungkyunkwan University (SKKU), Suwon 16419, Republic of Korea; SKKU Institute of Energy Science and Technology (SIEST), Sungkyunkwan University, Suwon 16419, Republic of Korea*

Hong Gu Kang − *Department of Materials Science and Engineering, Myongji University, Yongin 17058, Republic of Korea*

Minsu Kim − *Department of Advanced Materials Engineering, Kyonggi University, Suwon 16227, Republic of Korea*

Jaehoon Lim − *Department of Energy Science and Center for Artificial Atoms, Sungkyunkwan University (SKKU), Suwon 16419, Republic of Korea; SKKU Institute of Energy Science and Technology (SIEST), Sungkyunkwan University, Suwon 16419, Republic of Korea;* orcid.org/0000-0003-2623-3550

Complete contact information is available at: https://pubs.acs.org/10.1021/acsanm.3c01485

Author Contributions

The manuscript was written through contributions of all authors. Prof. S.-Y.C. designed and supervised this work and wrote the draft of the manuscript. E.A.K. and H.G.K. carried out the device fabrication and conducted optical analysis. J.H. and Prof. J.L. synthesized Cd-based QDs. Prof. M.K. conducted UPS analysis for energy band consideration. All authors have given approval to the final version of the manuscript.

Notes

The authors declare no competing financial interest.

ACKNOWLEDGMENTS

This work was supported by the National Research Foundation (NRF) funded by the Korean Government (NRF-2022R1A4A3018802, NRF-2021M3H4A3A01062964, and NRF-2021R1F1A1047892). This research was also supported by the Nano·Material Technology Development Program through the National Research Foundation of Korea (NRF) funded by the Ministry of Science, ICT and Future Planning (2009-0082580).

REFERENCES

(1) Shirasaki, Y.; Supran, G. J.; Bawendi, M. G.; Bulović, V. Emergence of Colloidal Quantum-Dot Light-Emitting Technologies. *Nat. Photonics* **2013**, *7*, 13−23.

(2) Jiang, Y.; Cho, S.-Y.; Shim, M. Light-Emitting Diodes of Colloidal Quantum Dots and Nanorod Heterostructures for Future Emissive Displays. *J. Mater. Chem. C* **2018**, *6*, 2618−2634.

(3) Pietryga, J. M.; Park, Y.-S.; Lim, J.; Fidler, A. F.; Bae, W. K.; Brovelli, S.; Klimov, V. I. Spectroscopic and Device Aspects of Nanocrystal Quantum Dots. *Chem. Rev.* **2016**, *116*, 10513−10622.
(4) Kagan, C. R.; Bassett, L. C.; Murray, C. B.; Thompson, S. M. Colloidal Quantum Dots as Platforms for Quantum Information Science. *Chem. Rev.* **2021**, *121*, 3186−3233.
(5) Alivisatos, A. P. Semiconductor Clusters, Nanocrystals, and Quantum Dots. *Science* **1996**, *271*, 933−937.
(6) Hahm, D.; Chang, J. H.; Jeong, B. G.; Park, P.; Kim, J.; Lee, S.; Choi, J.; Kim, W. D.; Rhee, S.; Lim, J.; Lee, D. C.; Lee, C.; Char, K.; Bae, W. K. Design Principle for Bright, Robust, and Color-Pure InP/ZnSexS1−x/ZnS Heterostructures. *Chem. Mater.* **2019**, *31*, 3476−3484.
(7) Bae, W. K.; Nam, M. K.; Char, K.; Lee, S. Gram-Scale One-Pot Synthesis of Highly Luminescent Blue Emitting Cd1−xZnxS/ZnS Nanocrystals. *Chem. Mater.* **2008**, *20*, 5307−5313.
(8) Yang, J.; Kee Choi, M.; Jeong Yang, U.; Young Kim, S.; Seong Kim, Y.; Hyun Kim, J.; Kim, D.-H.; Hyeon, T. Toward Full-Color Electroluminescent Quantum Dot Displays. *Nano Lett.* **2021**, *21*, 26−33.
(9) Lim, J.; Jeong, B. G.; Park, M.; Kim, J. K.; Pietryga, J. M.; Park, Y.-S.; Klimov, V. I.; Lee, C.; Lee, D. C.; Bae, W. K. Influence of Shell Thickness on the Performance of Light-Emitting Devices Based on CdSe/Zn1-XCdXS Core/Shell Heterostructured Quantum Dots. *Adv. Mater.* **2014**, *26*, 8034−8040.
(10) Song, J.; Wang, O.; Shen, H.; Lin, Q.; Li, Z.; Wang, L.; Zhang, X.; Li, L. S. Over 30% External Quantum Efficiency Light-Emitting Diodes by Engineering Quantum Dot-Assisted Energy Level Match for Hole Transport Layer. *Adv. Funct. Mater.* **2019**, *29*, No. 1808377.
(11) Qian, L.; Zheng, Y.; Xue, J.; Holloway, P. H. Stable and Efficient Quantum-Dot Light-Emitting Diodes Based on Solution-Processed Multilayer Structures. *Nat. Photonics* **2011**, *5*, 543−548.
(12) Bae, W. K.; Park, Y. S.; Lim, J.; Lee, D.; Padilha, L. A.; McDaniel, H.; Robel, I.; Lee, C.; Pietryga, J. M.; Klimov, V. I. Controlling the Influence of Auger Recombination on the Performance of Quantum-Dot Light-Emitting Diodes. *Nat. Commun.* **2013**, *4*, 2661.
(13) Oh, N.; Kim, B. H.; Cho, S. Y.; Nam, S.; Rogers, S. P.; Jiang, Y.; Flanagan, J. C.; Zhai, Y.; Kim, J. H.; Lee, J.; Yu, Y.; Cho, Y. K.; Hur, G.; Zhang, J.; Trefonas, P.; Rogers, J. A.; Shim, M. Double-Heterojunction Nanorod Light-Responsive LEDs for Display Applications. *Science* **2017**, *355*, 616−619.
(14) Pejović, V.; Georgitzikis, E.; Lee, J.; Lieberman, I.; Cheyns, D.; Heremans, P.; Malinowski, P. E. Infrared Colloidal Quantum Dot Image Sensors. *IEEE Trans. Electron Devices* **2022**, *69*, 2840−2850.
(15) Kong, L.; Wu, J.; Li, Y.; Cao, F.; Wang, F.; Wu, Q.; Shen, P.; Zhang, C.; Luo, Y.; Wang, L.; Turyanska, L.; Ding, X.; Zhang, J.; Zhao, Y.; Yang, X. Light-Emitting Field-Effect Transistors with EQE over 20% Enabled by a Dielectric-Quantum Dots-Dielectric Sandwich Structure. *Sci. Bull.* **2022**, *67*, 529−536.
(16) Kim, J.; Jo, C.; Kim, M.-G.; Park, G.-S.; Marks, T. J.; Facchetti, A.; Park, S. K. Vertically Stacked Full Color Quantum Dots Phototransistor Arrays for High-Resolution and Enhanced Color-Selective Imaging. *Adv. Mater.* **2022**, *34*, No. 2106215.
(17) Zhang, H.; Su, Q.; Chen, S. Quantum-Dot and Organic Hybrid Tandem Light-Emitting Diodes with Multi-Functionality of Full-Color-Tunability and White-Light-Emission. *Nat. Commun.* **2020**, *11*, 2826.
(18) Jang, E.; Jun, S.; Jang, H.; Lim, J.; Kim, B.; Kim, Y. White-Light-Emitting Diodes with Quantum Dot Color Converters for Display Backlights. *Adv. Mater.* **2010**, *22*, 3076−3080.
(19) Bae, W. K.; Lim, J.; Lee, D.; Park, M.; Lee, H.; Kwak, J.; Char, K.; Lee, C.; Lee, S. R/G/B/Natural White Light Thin Colloidal Quantum Dot-Based Light-Emitting Devices. *Adv. Mater.* **2014**, *26*, 6387−6393.
(20) Han, C.-Y.; Yoon, S.-Y.; Lee, S.-H.; Song, S.-W.; Jo, D.-Y.; Jo, J.-H.; Kim, H.-M.; Kim, H.-S.; Yang, H. High-Performance Tricolored White Lighting Electroluminescent Devices Integrated with Environmentally Benign Quantum Dots. *Nanoscale Horiz.* **2021**, *6*, 168−176.
(21) Kim, J. H.; Lee, K. H.; Kang, H. D.; Park, B.; Hwang, J. Y.; Jang, H. S.; Do, Y. R.; Yang, H. Fabrication of a White Electroluminescent Device Based on Bilayered Yellow and Blue Quantum Dots. *Nanoscale* **2015**, *7*, 5363.
(22) Zhang, H.; Wang, S.; Sun, X.; Chen, S. All Solution-Processed White Quantum-Dot Light-Emitting Diodes with Three-Unit Tandem Structure. *J. Soc. Inf. Disp.* **2017**, *25*, 143−150.
(23) Jiang, C.; Zou, J.; Liu, Y.; Song, C.; He, Z.; Zhong, Z.; Wang, J.; Yip, H.-L.; Peng, J.; Cao, Y. Fully Solution-Processed Tandem White Quantum-Dot Light-Emitting Diode with an External Quantum Efficiency Exceeding 25%. *ACS Nano* **2018**, *12*, 6040−6049.
(24) Lim, J.; Park, Y. S.; Wu, K.; Yun, H. J.; Klimov, V. I. Droop-Free Colloidal Quantum Dot Light-Emitting Diodes. *Nano Lett.* **2018**, *18*, 6645−6653.
(25) Hong, A.; Kim, J.; Kwak, J. Sunlike White Quantum Dot Light-Emitting Diodes with High Color Rendition Quality. *Adv. Opt. Mater.* **2020**, *8*, No. 2001051.
(26) Lee, T.; Kim, B. J.; Lee, H.; Hahm, D.; Bae, W. K.; Lim, J.; Kwak, J. Bright and Stable Quantum Dot Light-Emitting Diodes. *Adv. Mater.* **2022**, *34*, No. 2106276.
(27) Lee, K.-H.; Han, C.-Y.; Kang, H.-D.; Ko, H.; Lee, C.; Lee, J.; Myoung, N.; Yim, S.-Y.; Yang, H. Highly Efficient, Color-Reproducible Full-Color Electroluminescent Devices Based on Red/Green/Blue Quantum Dot-Mixed Multilayer. *ACS Nano* **2015**, *9*, 10941−10949.
(28) Ki Bae, W.; Kwak, J.; Lim, J.; Lee, D.; Ki Nam, M.; Char, K.; Lee, C.; Lee, S. Multicolored Light-Emitting Diodes Based on All-Quantum-Dot Multilayer Films Using Layer-by-Layer Assembly Method. *Nano Lett.* **2010**, *10*, 2368−2373.
(29) Lee, K.-H.; Han, C.-Y.; Jang, E.-P.; Jo, J.-H.; Hong, S.; Hwang, J. Y.; Choi, E.; Hwang, J.-H.; Yang, H. Full-Color Capable Light-Emitting Diodes Based on Solution-Processed Quantum Dot Layer Stacking. *Nanoscale* **2018**, *10*, 6300−6305.
(30) Wang, L.; Pan, J.; Qian, J.; Lei, W.; Wu, Y.; Zhang, W.; Goto, D. K.; Chen, J. A Highly Efficient White Quantum Dot Light-Emitting Diode Employing Magnesium Doped Zinc Oxide as the Electron Transport Layer Based on Bilayered Quantum Dot Layers. *J. Mater. Chem. C* **2018**, *6*, 8099−8104.
(31) Wu, Q.; Gong, X.; Zhao, D.; Zhao, Y.-B.; Cao, F.; Wang, H.; Wang, S.; Zhang, J.; Quintero-Bermudez, R.; Sargent, E. H.; Yang, X. Efficient Tandem Quantum-Dot LEDs Enabled by An Inorganic Semiconductor-Metal-Dielectric Interconnecting Layer Stack. *Adv. Mater.* **2022**, *34*, No. 2108150.
(32) Cao, F.; Zhao, D.; Shen, P.; Wu, J.; Wang, H.; Wu, Q.; Wang, F.; Yang, X. High-Efficiency, Solution-Processed White Quantum Dot Light-Emitting Diodes with Serially Stacked Red/Green/Blue Units. *Adv. Opt. Mater.* **2018**, *6*, No. 1800652.
(33) Kim, G.-H.; Lee, J.; Lee, J. Y.; Han, J.; Choi, Y.; Kang, C. J.; Kim, K.-B.; Lee, W.; Lim, J.; Cho, S.-Y. High-Resolution Colloidal Quantum Dot Film Photolithography via Atomic Layer Deposition of ZnO. *ACS Appl. Mater. Interfaces* **2021**, *13*, 43075−43084.
(34) Lee, J. Y.; Kim, E. A.; Han, J.; Choi, Y.-H.; Hahm, D.; Kang, C. J.; Bae, W. K.; Lim, J.; Cho, S.-Y. Nondestructive Direct Photolithography for Patterning Quantum Dot Films by Atomic Layer Deposition of ZnO. *Adv. Mater. Interfaces* **2022**, *9*, No. 2200835.
(35) Borg, L. Z.; Lee, D.; Lim, J.; Bae, W. K.; Park, M.; Lee, S.; Lee, C.; Char, K.; Zentel, R. The Effect of Band Gap Alignment on the Hole Transport from Semiconducting Block Copolymers to Quantum Dots. *J. Mater. Chem. C* **2013**, *1*, 1722−1726.
(36) Kim, G.-H.; Noh, K.; Han, J.; Kim, M.; Oh, N.; Lee, W.; Na, H. B.; Shin, C.; Yoon, T.-S.; Lim, J.; Cho, S.-Y. Enhanced Brightness and Device Lifetime of Quantum Dot Light-Emitting Diodes by Atomic Layer Deposition. *Adv. Mater. Interfaces* **2020**, *7*, No. 2000343.
(37) Cho, S.-Y.; Oh, N.; Nam, S.; Jiang, Y.; Shim, M. Enhanced Device Lifetime of Double-Heterojunction Nanorod Light-Emitting Diodes. *Nanoscale* **2017**, *9*, 6103−6110.
(38) Wu, S.; Han, S.; Zheng, Y.; Zheng, H.; Liu, N.; Wang, L.; Cao, Y.; Wang, J. PH-Neutral PEDOT:PSS as Hole Injection Layer in Polymer Light Emitting Diodes. *Org. Electron.* **2011**, *12*, 504−508.

https://doi.org/10.1021/acsanm.3c01485
ACS Appl. Nano Mater. 2023, 6, 11455−11464

(39) Jin, H.; Moon, H.; Lee, W.; Hwangbo, H.; Yong, S. H.; Chung, H. K.; Chae, H. Charge Balance Control of Quantum Dot Light Emitting Diodes with Atomic Layer Deposited Aluminum Oxide Interlayers. *RSC Adv.* **2019**, *9*, 11634−11640.
(40) Dai, X.; Zhang, Z.; Jin, Y.; Niu, Y.; Cao, H.; Liang, X.; Chen, L.; Wang, J.; Peng, X. Solution-Processed, High-Performance Light-Emitting Diodes Based on Quantum Dots. *Nature* **2014**, *515*, 96−99.
(41) Chang, J. H.; Park, P.; Jung, H.; Jeong, B. G.; Hahm, D.; Nagamine, G.; Ko, J.; Cho, J.; Padilha, L. A.; Lee, D. C.; Lee, C.; Char, K.; Bae, W. K. Unraveling the Origin of Operational Instability of Quantum Dot Based Light-Emitting Diodes. *ACS Nano* **2018**, *12*, 10231−10239.
(42) Lee, H.; Jeong, B. G.; Bae, W. K.; Lee, D. C.; Lim, J. Surface State-Induced Barrierless Carrier Injection in Quantum Dot Electroluminescent Devices. *Nat. Commun.* **2021**, *12*, 5669.

https://doi.org/10.1021/acsanm.3c01485
ACS Appl. Nano Mater. 2023, 6, 11455−11464